Lawrence Berkeley National Laboratory
Recent Work

Title
THE VISCOSITY OP LIQUID CESIUM UP TO l6OO C

Permalink
https://escholarship.org/uc/item/7sp5f1sf

Authors
Tsai, H.C.
Olander, D.R.

Publication Date
1973-08-01

THE VISCOSITY OF LIQUID CESIUM UP TO 1600°C

H. C. Tsai and D. R. Olander

August 1973

DISCLAIMER

THE VISCOSITY OF LIQUID CESIUM UP TO 1600°C

H. C. Tsai[*] and D. R. Olander
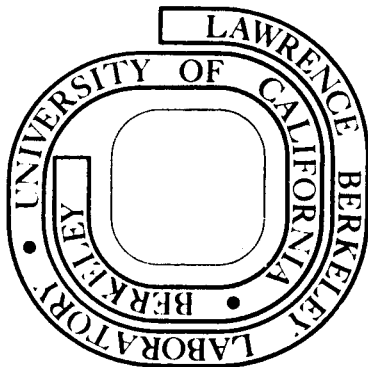
Inorganic Materials Research Division, Lawrence Berkeley Laboratory
and Department of Nuclear Engineering, University of California,
Berkeley, California 94720

ABSTRACT

The viscosity of liquid cesium has been measured up to 1600°C by oscillating cup technique. The results can be represented by the equations

$$\ln \eta(mP) = -0.187 + \frac{6.34 \times 10^2}{T}, \quad 410°K \leq T \leq 1100°K,$$

$$\ln \eta(mP) = -2.55 + \frac{6.01 \times 10^3}{T} - \frac{3.10 \times 10^6}{T^2}, \quad 1100°K < T < 1900°K.$$

The critical viscosity of cesium determined from the law of rectilinear diameters is 0.57 ± 0.04 millipoise. Viscosities of sodium and potassium were also estimated from the cesium data by the law of corresponding states.

* Present address: Argonne National Laboratory, Argonne, Illinois.

INTRODUCTION

Alkali metals are of interest as high temperature coolants and working fluids in many nuclear and space applications. Viscosity is one of the transport properties which are required for rational design of systems involving alkali metals for such applications.

Among the numerous techniques for viscosity measurements, oscillating cup viscometry was adopted for the present study of cesium viscosity. The viscometer is a cylindrical crucible containing the fluid and suspended by a wire. Torsional oscillation about the vertical axis, initiated by a twist of the suspension wire, is damped by the viscous drag of the fluid inside. The theory of oscillating cup viscometer is discussed in refs. (1)-(3).

The crucible used in the oscillating cup technique has essentially a constant volume and because of the thermal expansion of the sample fluid, complete filling of the crucible with the liquid is not possible if one sample is to be studied over a range of temperatures. As a result, there is always a space in the crucible on top of the liquid phase which is occupied by the saturated vapor. For low temperature experiments, the viscous drag due to the vapor phase is negligible. This condition is not valid at high temperatures when the vapor pressure of the liquid is large enough to render the mean free path in the gas less than the crucible dimensions. In addition to the high vapor pressure, the temperature dependences of the liquid and vapor viscosities accentuate the effect of vapor drag on crucible motion. The liquid viscosity decreases with temperature owing to the positive activation energy of this transport property, but the vapor viscosity increases

with temperature due to the increased translational momentum transfer.
The liquid and vapor viscosities approach each other at high temperature
and eventually become equal at the critical point (4). For this reason,
a two-phase solution to the fluid mechanics of the oscillating cup
viscometer was developed and employed in the present study. (See
appendix.)

Cesium was chosen for study for the following reasons:

(a) It has the lowest critical temperature and pressure of all of
the alkali metals (5).

(b) Its critical constants and liquid and saturated vapor densities
have been measured (5).

(c) It is compatible with tungsten (the crucible material) up to
the critical temperature (6).

The viscosities of the alkali metals have been calculated (7).

EXPERIMENTAL APPARATUS

The system shown in Fig. 1 is similar to those employed in refs.
(8) and (9). The pendulum is made up of five parts: the crucible (D),
in which the sample is held, the support rod (E), the thermal insulator
(F), the inertial portion of the pendulum (G), and the chuck (H). A
photograph of the assembly is shown in Fig. 2. A polished surface on
(G) is used to reflect the incident laser light (Z) by which the
oscillatory motion is monitored. This portion also has a horizontal
hole into which different inertia rods (I) can be inserted so that the
moment of inertia of the pendulum can be adjusted.

The pendulum system is suspended by a piece of torsion fibre (J).
The wire is attached to a second chuck (K) which is fixed to a rotatable
holder (L). The holder, which rests on a supporting plate (M) is
attached mechanically to a rotary feedthrough (N) by which oscillation
of the pendulum is initiated through the vacuum wall.

The crucible is suspended in the hot zone of a Brew tungsten mesh
furnace (A) of 4.4 cm diameter and 8.9 cm height. Layers of tungsten
thermal shields arranged on the side, the top, and the bottom reduce the
radiation heat loss and also provide uniform temperature in the hot zone.
Temperatures up to 1300°C are measured by a chromel-alumel thermocouple
located close to the crucible. An optical pyrometer (P) which sighted
through a right angle prism (Q) into a hole 0.32 cm in diameter drilled
through the bottom shield parts into the inner furnace region is used
to measure temperatures above 900°C.

The entire system is enclosed in a vacuum tank (C) evacuated by two
liquid nitrogen sorption pumps (SP). The pressure ($<3 \times 10^{-5}$ torr)
maintained by the sorption pumps is low enough that additional pumping
is unnecessary.

Since the vapor pressure of cesium increases sharply as the critical
temperature is approached whereas the strength of tungsten decreases
rapidly with temperature, two kinds of crucibles were employed. The
"thin-wall" type shown in Fig. 3 was used for low temperature runs.
Figure 4 shows the "pressure vessel" type crucibles used for high
temperature, high pressure runs. Because of the combination of low
moment of inertia and high specimen viscosity, the thin-wall crucible
provides higher precision data than the bulkier high pressure design.

The pendulum motion recording system is illustrated in Fig. 5.

The laser spot reflected from the polished surface on the pendulum triggers a photocell located in the vacuum chamber. Before feeding the output of the photocell to the multichannel analyzer, a logic circuit corrects the spatial error due to the finite dimensions of the photocell and laser beam. Due to the finite time ($\sim$ msec) required for the laser spot to pass the photocell, the width of the output from the photocell increases as the oscillation motion slows down. The logic circuit generates a narrow pulse ($\sim$ 1 μsec width) each time the laser beam passes the edge of the photocell (either one) which is used as the reference position.

The shaped pulses are used as the channel advancing pulses to the multichannel analyzer operating in the multiscalar mode. At the same time, 100 KHz timing pulses are fed into the analyzer. The counting starts at channel 1 and continues until a channel advancing pulse transfers the timing pulses to channel 2 and so on. Since each count is equivalent to 10 μsec, the number of timing pulses stored in a particular channel provides an accurate measure of the time elapsed between successive passages of the beam past the photocell. Figure 6 shows a typical set of data obtained with this system.

The position of the photocell is, in general, different from that of the reflected light beam with the pendulum in equilibrium (i.e. not oscillating). The upper points, T_1, T_3, T_5, etc. in Fig. 6 represent the time intervals for the pendulum to move from the photocell to the maximum angular displacement farthest from the photocell and return to the cell. The lower points, T_2, T_4, T_6, etc., are a similar record for the remaining portion of the oscillation. From these time intervals,

the decay constant β of the pendulum motion may be calculated by the
formula

$$\beta = \frac{1}{2\pi} \, \ell n \left[\frac{\cos\left(\frac{\pi T_3}{\tau}\right)}{\cos\left(\frac{\pi T_1}{\tau}\right)} \right].$$

The period τ is obtained from the same data.

EXPERIMENTAL PROCEDURE

The high purity (99.99%) cesium metal was supplied by Leico
Industries, Inc. in sealed glass ampoules.

Tungsten crucibles and cesium were loaded in a glove box flushed
with dry nitrogen. The cesium was melted and poured into the crucible.
The amount loaded was roughly controlled by measuring the weight increase
of the crucible using the balance inside the glove box. To prevent
overheating of the cesium metal during electron beam welding, the crucible
was held inside a heat sink consisting of a copper block prechilled to
liquid nitrogen temperature. This method effectively eliminated the
vaporization of cesium during welding but increased the frequency of
cracking in the weld due to the large thermal gradient. After the lid
was electron-beam welded to the body, the exact weight of the cesium
charge was accurately measured by an analytic balance.

The intrinsic damping of the oscillating system was measured before
each series of experiments while the sample was solid. The temperature
was then increased in a stepwise manner and damping of the crucible with
the sample liquid was measured. Between each
measurement at different temperatures, a braking device was engaged to

bring the pendulum system completely to rest before an initial twist was

given to the pendulum. In each experiment, 25 consecutive oscillations

were recorded and used to determine the mean period and decay constant.

After the series of experiments was terminated, the intrinsic decay

constant was measured again to reaffirm the value measured prior to the

experiments. The temperature dependence of the intrinsic damping was

determined separately with a dummy crucible (consisting of solid tung-

sten). It was found to be independent of specimen temperature in the

experimental range.

RESULTS

The cesium viscosity measurements were carried out with two thin-

wall crucibles (A and B) in the temperature range from 135 to 550°C and

from 530°C to 815°C, respectively, and with one pressure vessel type

crucible (D) from 800 to 1600°C. Slight overlap of the temperature

ranges provided a check of the consistency of data obtained from different

viscometers. The characteristics of these three viscometers are given

in Table I.

Two-phase solution was employed for temperatures greater than 600°C,

at which temperature the reported vapor viscosity is about 1/8 of that

of the liquid. The difference between values of the liquid viscosity

deduced from the set of data but analyzed by the single-phase and two-

phase solutions of the equations of motion depends on the temperature

and the relative height of the vapor phase compared to that of the

liquid. With viscometer B at 600°C, the corrected liquid viscosity is

8% less than that without the correction for vapor drag. For crucible D

at 1600°C, the analogous figure is 30%.

Figure 7 shows the measured cesium viscosity along with the results

of Achener and Boyer (10), who measured the cesium viscosity using the

oscillating cup technique up to 1060°C. The agreement between two sets

of data is quite good.

DISCUSSION

Law of Rectilinear Diameters: The Critical Viscosity of Cesium

The fact that the viscosity varies rapidly as the critical tempera-

ture is approached coupled with the problem of accurately loading the

amount of sample required to achieve the critical state makes the direct

measurement of critical viscosity very difficult. Cailletet and Mathias

(11) first discovered that when approaching the critical temperature,

the mean density of the liquid and its saturated vapor is approximately

a linear function of temperature. Grosse later pointed out that this

law of "rectilinear diameters" also applies to viscosities (4). This

procedure was utilized to estimate the critical viscosity from the

present liquid phase data and Bonilla's (7) vapor phase calculations.

Since the points for both phases extend quite close to the critical

point, the accuracy of such an extrapolation is good.

The mean viscosity calculated from the data between 1200 and 1600°C

is shown in Fig. 8. In this temperature range, the mean viscosity is a

very good linear function of temperature. Extrapolating the mean vis-

cosity to 1760°C, the reported critical temperature of cesium (5),

yields a critical viscosity of 0.57 ± 0.04 millipoise. This value is

smaller than the 0.8 millipoise Grosse obtained by extrapolation of

estimated sodium and potassium critical viscosities (4).

Theory of Corresponding States: Viscosities of Sodium and Potassium

The high pressure limitation discussed in the introduction means that viscosity measurements covering the entire liquid range of the other alkali metals might not be experimentally feasible for some time to come. Because of their high critical pressures, lithium, sodium and potassium are even more difficult to contain near the critical point than is cesium. Consequently, we estimate the critical viscosities of the other alkali metals from our cesium data by using the theory of corresponding states.

One of the conditions for the applicability of the principle of corresponding states to a class of substances is that the reduced interatomic potential energy be a universal function of the reduced interatomic distance (i.e. $\frac{\mu}{\epsilon} = \mu(\frac{r}{\sigma})$, where ϵ and σ are the force constants of the potential function). The similarity in the properties of the alkali metals should satisfy this requirement quite well. The law of corresponding states suggests that there is a unique functional dependence of the reduced viscosity on reduced temperature and volume (12)(13), or:

$$\eta^* = \eta^* (T^*, V^*) = \frac{\eta \sigma^2 N_0^{1/2}}{M^{1/2} \epsilon^{1/2}}$$

where

T^* = reduced temperature = $\frac{kT}{\epsilon}$,

V^* = reduced volume = $\frac{1}{n\sigma^3}$,

n = molecular density,

M = atomic weight,

N_o = Arogadro's number.

Because of the difficulty of determining the necessary values for σ, it is convenient to follow Pasternak's method (14) of multiplying η^* by $(V^*)^{2/3}$ to eliminate σ from the above equation. The resulting dimensionless quantity is

$$\eta^* (V^*)^{2/3} = \frac{\eta N_o^{1/3} V^{2/3}}{(MR \frac{\varepsilon}{k})^{1/2}} = f(T^*)$$

where R is the gas constant. The energy parameter $\frac{\varepsilon}{k}$ is determined from Chapman's (13) empirical relationship of

$$\frac{\varepsilon}{k} = 5.2\ T_m$$

where T_m is the melting point of the liquid metal in $^\circ K$.

The universal viscosity curve for the alkali metals (based upon cesium data) is shown in Fig. 9. The reduced viscosity of the alkali metals at the critical point is

$$\eta_c^* = 0.24$$

The sodium and potassium viscosities predicted from the universal plot of Fig. 9 are shown in Figs. 10 and 11, respectively, along with the experimental results of Kalakutskaya (15). The agreement is satisfactory at medium and high temperatures. With the vapor viscosity data provided by Bonilla and co-workers (7), law of rectilinear diameter may be used

to determine the following critical viscosities:

$$\eta_c = 0.50 \pm 0.05 \text{ millipoise for sodium}$$

and

$$\eta_c = 0.46 \pm 0.05 \text{ millipoise for potassium.}$$

ACKNOWLEDGMENTS

APPENDIX

The Motion of an Oscillating Crucible Containing Two Phases

After the transient part of the oscillation motion has decayed, the fluid velocity components in the radial and vertical directions may be set equal to zero and there is no velocity gradient in the angular direction. The Navier-Stokes equations can then be simplified to (3):

$$\frac{1}{\nu_\ell}\frac{\partial \psi_\ell}{\partial t} = \frac{\partial^2 \psi_\ell}{\partial r^2} + \frac{3}{r}\frac{\partial \psi_\ell}{\partial r} + \frac{\partial^2 \psi_\ell}{\partial Z^2} \qquad\qquad \text{(A-1a)}$$

and

$$\frac{1}{\nu_v}\frac{\partial \psi_v}{\partial t} = \frac{\partial^2 \psi_v}{\partial r^2} + \frac{3}{r}\frac{\partial \psi_v}{\partial r} + \frac{\partial^2 \psi_v}{\partial Z^2} \qquad\qquad \text{(A-1b)}$$

Since the fluid and the crucible have the same oscillating period τ and decay constant β, the time and spatial components of the angular velocities may be written as:

$$\psi_\ell \ (r,Z,t) = \Phi_\ell(r,Z)e^{\alpha t} \qquad\qquad \text{(A-2a)}$$

$$\psi_v \ (r,Z,t) = \Phi_v(r,Z)e^{\alpha t} \qquad\qquad \text{(A-2b)}$$

where $\alpha = -\beta + i\gamma$ and γ is defined as $2\pi/\tau$. From Eqs. (A-1) and (A-2), the equations of motion reduce to:

$$\frac{\alpha}{\nu_\ell} \, \Phi_\ell = \frac{\partial^2 \Phi_\ell}{\partial r^2} + \frac{3}{r} \, \frac{\partial \Phi_\ell}{\partial r} + \frac{\partial^2 \Phi_\ell}{\partial Z^2} \qquad \text{(A-3a)}$$

$$\frac{\alpha}{\nu_v} \, \Phi_v = \frac{\partial^2 \Phi_v}{\partial r^2} + \frac{3}{r} \, \frac{\partial \Phi_v}{\partial r} + \frac{\partial^2 \Phi_v}{\partial Z^2} \qquad \text{(A-3b)}$$

Equations (A-3a) and (A-3b) are subject to the following boundary conditions:

(I) $\Phi_\ell = \Phi_o$ at r=a and Z=0,

(II) $\Phi_v = \Phi_o$ at r=a and Z=H,

(III) $\Phi_\ell = \Phi_v$ at Z=h,

(IV) $\eta_\ell \, \dfrac{\partial \Phi_\ell}{\partial Z} = -\eta_v \, \dfrac{\partial \Phi_v}{\partial Z}$ at Z=h,

where Φ_o is the angular velocity of the crucible as it passes the equilibrium position, η_ℓ and η_v are the dynamic viscosities of the liquid and saturated vapor, respectively, αa is the inside diameter of the crucible, H is the height of the crucible and h is the height of the liquid phase. Condition (III) assumes no slip at the interface and condition (V) represents the continuity of the shear stress at the interface.

The solutions of Eqs. (A-3a) and (A-3b) are

$$\Phi_\ell = \sum_{n=1}^{\infty} [A_n^\ell \sinh \ \ell_n^\ell \ Z + B_n^\ell \cosh \ \ell_n^\ell \ (h-Z)]$$

$$\frac{J_1(\kappa_n r)}{r} + \frac{a\Phi_o}{r} \frac{J_1(m_\ell r)}{J_1(m_\ell a)} \tag{A-4a}$$

and

$$\Phi_v = \sum_{n=1}^{\infty} [A_n^v \sin h \ \ell_n^v \ z + B_n^v \cos h \ \ell_n^v \ (H-h-z)]$$

$$\frac{J_1(\kappa_n r)}{r} + \frac{a\Phi_o}{r} \frac{J_1(m_v r)}{J_1(m_v a)} \tag{A-4b}$$

where J_1 is the Bessel function of order one and

$$J_1(\kappa_n a) = 0,$$

$$m_\ell^2 = -\frac{\alpha}{\nu_\ell},$$

$$m_v^2 = -\frac{\alpha}{\nu_v},$$

$$(\ell_n^\ell)^2 = \kappa_n^2 - m_\ell^2,$$

$$(\ell_n^v)^2 = \kappa_n^2 - m_v^2 \; ,$$

$$B_n^\ell = \frac{2 \, m_\ell^2 \, \Phi_o}{J_2(\kappa_n a)\kappa_n \, (\ell_n^\ell)^2 \, \cosh \, (\ell_n^\ell h)} \; ,$$

$$B_n^v = \frac{2m_v^2 \, \Phi_o}{J_2(\kappa_n a) \, \kappa_n \, (\ell_n^v)^2 \, \cosh \, [\ell_n^v (H-h)]} \; ,$$

$$A_n^\ell = \left\{ - \frac{2\kappa_n^2}{(\ell_n^\ell)^2} + \frac{2\kappa_n^2}{(\ell_n^v)^2} - \frac{2m_\ell^2}{(\ell_n^\ell)^2 \, \cosh \, (\ell_n^\ell h)} + \frac{2m_v^2}{(\ell_n^v)^2 \, \cosh \, [\ell_n^v (H-h)]} \right\} \Phi_o$$

$$J_2 (\kappa_n a) \, \kappa_n \, \sinh \, (\ell_n^\ell h) - \frac{\eta_\ell \ell_n^\ell}{\eta_v \ell_n^v} \, \cosh \, (\ell_n^\ell h) \, \tanh \, [\ell_n^v (H-h)] \; ,$$

$$A_n^v = \frac{\eta_\ell}{\eta_v} \, \frac{\ell_n^\ell}{\ell_n^v} \, \frac{\cosh \, (\ell_n^\ell h)}{\cosh \, [\ell_n^v (H-h)]} \, A_n^\ell$$

and

$$z = H - Z.$$

The damping coefficient L of the system can be determined from Eqs. (A-4a) and (A-4b) as a function of η_ℓ and η_v.

The equation of motion of a sinusodally damped oscillation is given by

$$I\alpha^2 + L\alpha + f = o \qquad\qquad (A-5)$$

where I = moment of inertia of the empty system, and

     f = spring constant of the torsion fibre.

To determine η_ℓ if η_v is known (or vice versa), the imaginary part of Eq. (A-5) is to be solved by trial and error. It is also possible to determine both η_ℓ and η_v from two measurements with different sample charges (i.e. different values of h).

REFERENCES

1. Roscoe, R., Proc. Phys. Soc. 72, 576 (1958).

2. Thresh, H. R., Trans. ASM 55, 790 (1962).

3. Hopkins, M. R. and Toye, T. C., Proc. Phys. Soc. 863, 773 (1950).

4. Grosse, A. V., Science 147, 1438 (1965).

5. Ross, R. G. and Greenwood, D. A., "Liquid Metals and Vapours Under Pressure," Pergamon Press, Oxford, 1970.

6. DeMastery, J. A. and Griesenauer, N. M., Met. Soc. Conf. Vol. 41, (1965), p. 1169.

7. Lee, C. S., Lee, D. I. and Bonilla, C. F., Nucl. Eng. Des. 10, 83 (1969).

8. Finucane, J. S. and Olander, D. R., Hi. Temp. Sci. 1, 466 (1969).

9. Tsai, H. C. and Olander, D. R., J. Nucl. Matls. 44, 83 (1972).

10. Achener, P. Y. and Boyer, M. R., AGN-8192, Vol. 3, Aerojet-General Nucleonics (1966).

11. Cailletet and Mathias, Compt. Rend. 102, 1202 (1886).

12. Helfand, E. and Rice, S., J. C. Phys. 32, 1642 (1960).

13. Chapman, T. W., A. I. Ch. E. J. 12, 395 (1966).

14. Pasternak, A. D., Phys. Ch. Liq. 3, 41 (1972).

15. Kalakutskaya, N. A., Hi. Temp. 6, 436 (1968).

Table I. Characteristics of Viscometers and Cesium Loadings

	A	B	D
Crucible Material	Tungsten	Tungsten	Tungsten
Torsion Wire	W-3% Re 0.018 cm diameter (Annealed)		
Crucible Type	thin wall	thin wall	pressure vessel
Crucible I.D. (cm)	1.58	1.58	1.59
Crucible Inside Height (cm)	6.05	6.04	5.59
Moment of Inertia (gm-cm^2)	274.62	275.84	397.33
Cesium Charge (gms)	15.593	10.035	7.044
Height of Liquid (cm)	4.44 at 500°C	3.68 at 815°C	4.05 at 1605°C
Temperature Range	135-550°C	530-815°C	800-1605°C

FIGURE CAPTIONS

Fig. 1. Sectional diagram of the experimental system.

Fig. 2. Torsion pendulum.

Fig. 3. Sectional view of the thin-wall crucible.

Fig. 4. Sectional view of the thick-wall crucible.

Fig. 5. Pendulum motion recording system.

Fig. 6. A typical set of data shown on the screen of the multi-channel
         analyzer.

Fig. 7. Liquid cesium viscosity.

Fig. 8. Law of rectilinear diameters of cesium metal (saturated vapor
         viscosities from ref. 7).

Fig. 9. Universal viscosity-temperature function for the alkali metals.

Fig. 10. Sodium viscosity calculated from the theory of corresponding
         states.

Fig. 11. Potassium viscosity calculated from the theory of correspond-
          ing states.
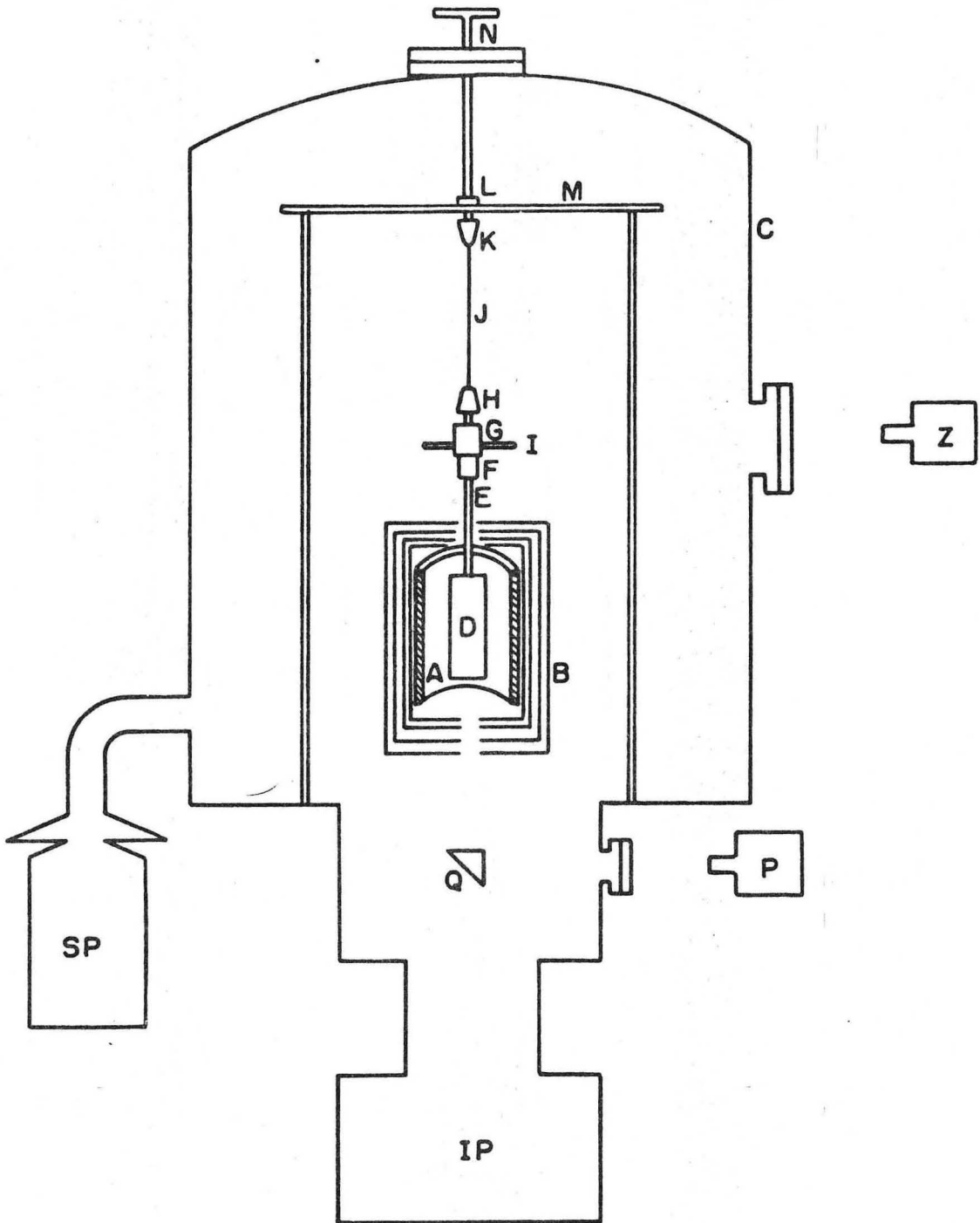
XBL 731 5639

Fig. 1

XBB 734-2475

Fig. 2

Connecting rod

Lips for
eb welding

1.58
cm

0.30
cm

6.02
cm

XBL734-2702

Fig. 3

Fig. 4

XBL734-2701

Mirrored Surface
on the Pendulum

He Gas
Laser

Photocell

Logic
Circuit

Multi-Channel
Analyzer

Pulse
Shaper

100 KHz
Sinewave
Generator

Counter
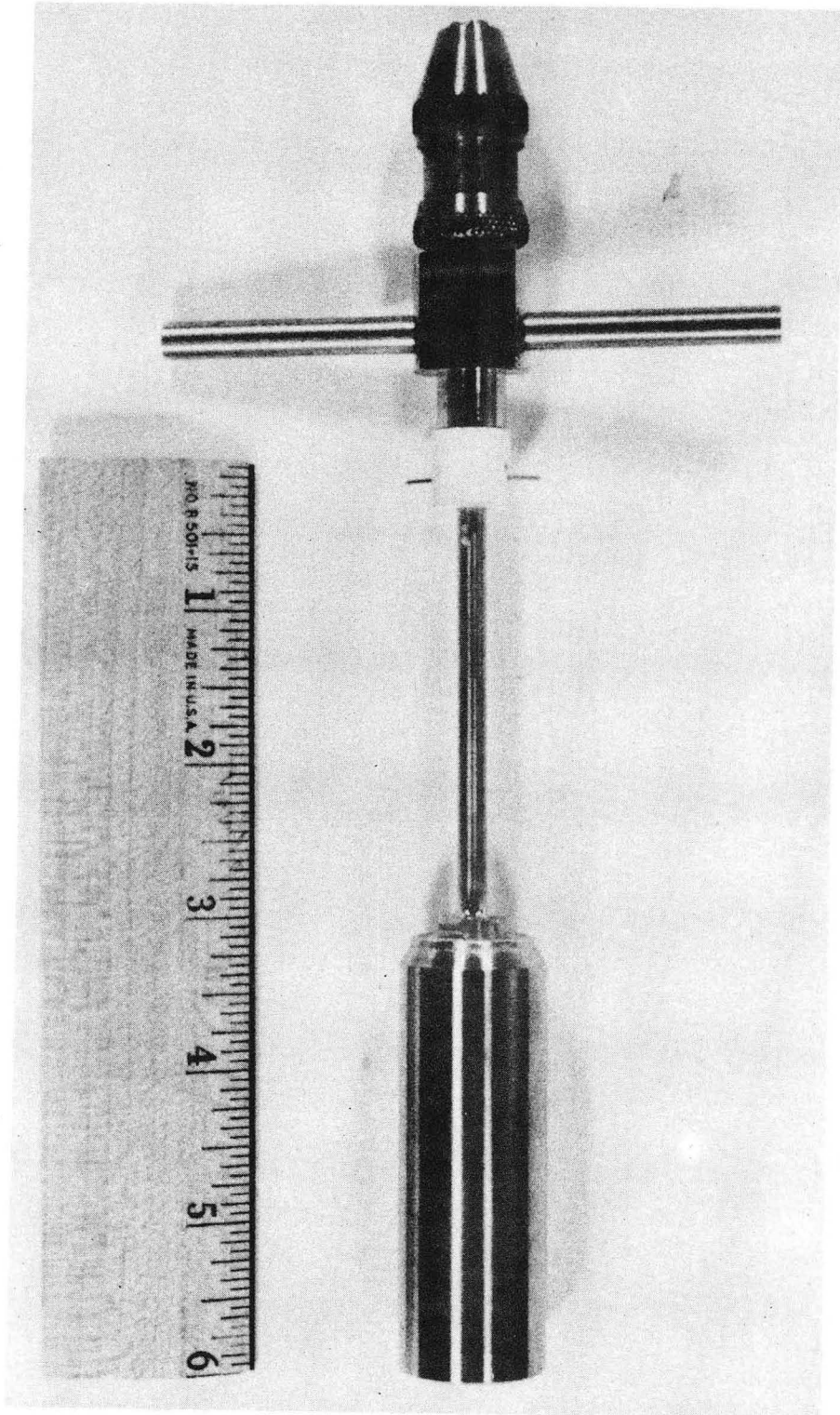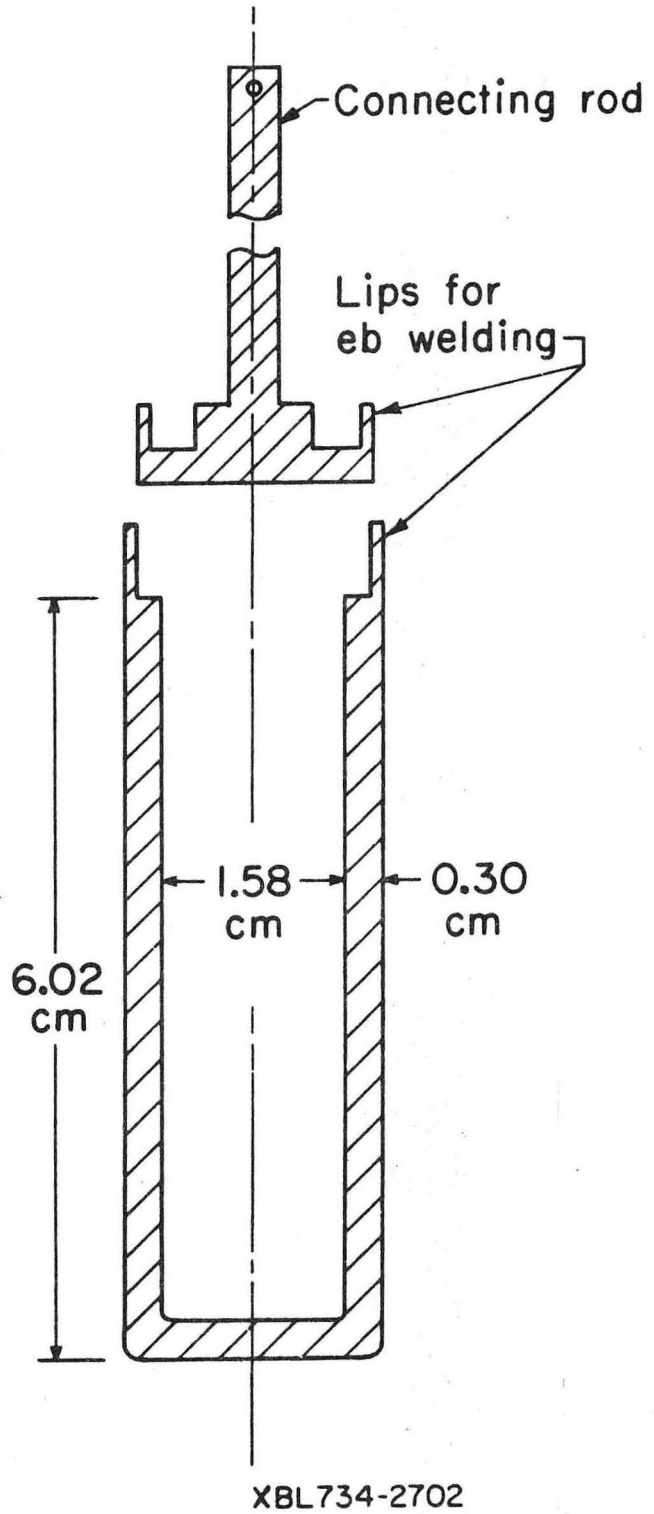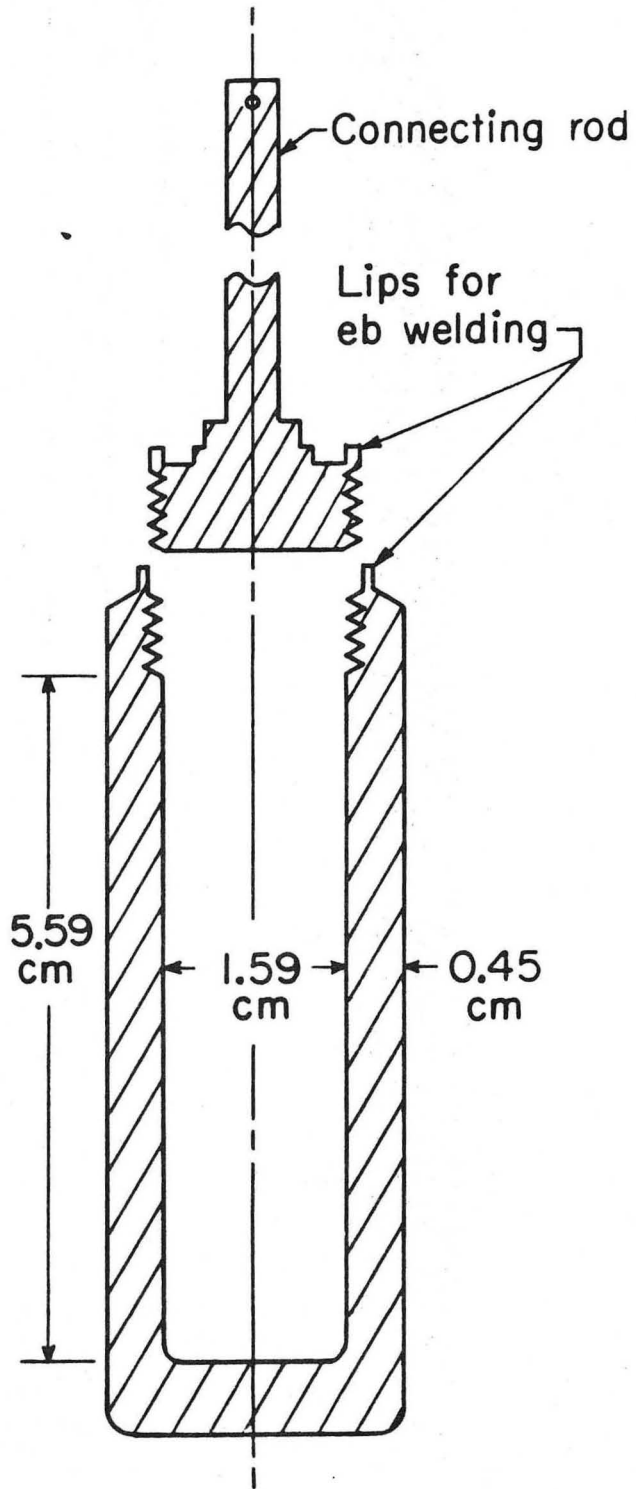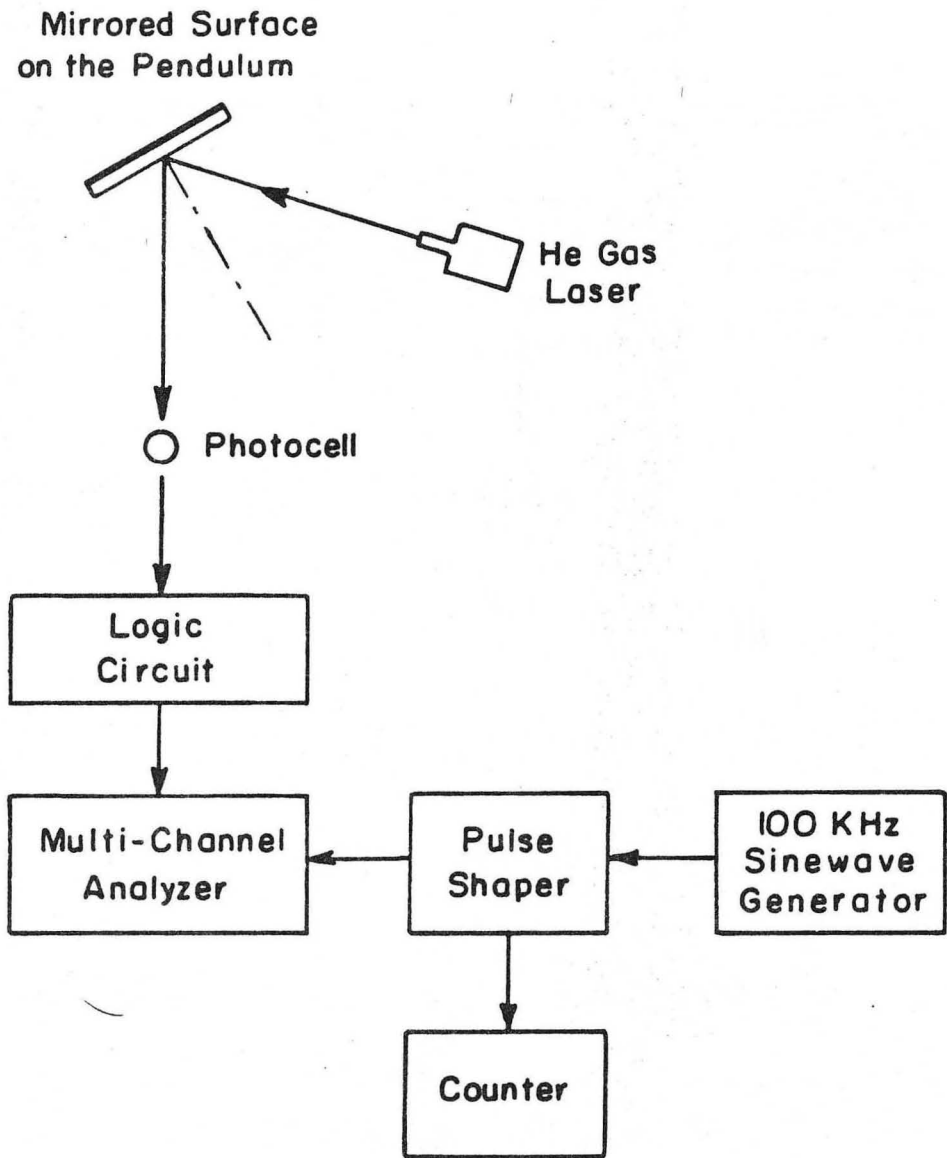
XBL731-5640

Fig. 5
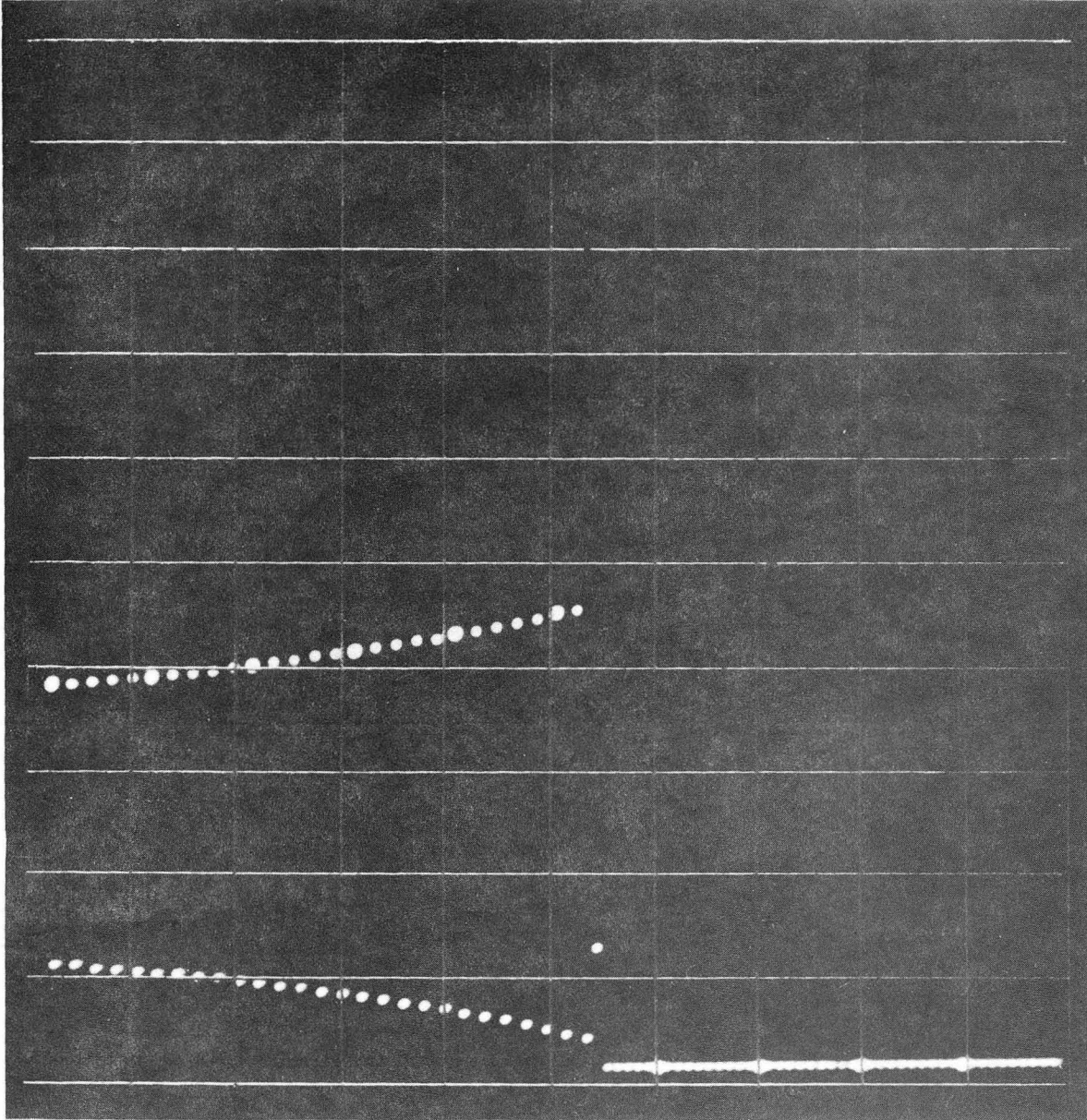
XBB 722-990

Fig. 6

XBL734-2703
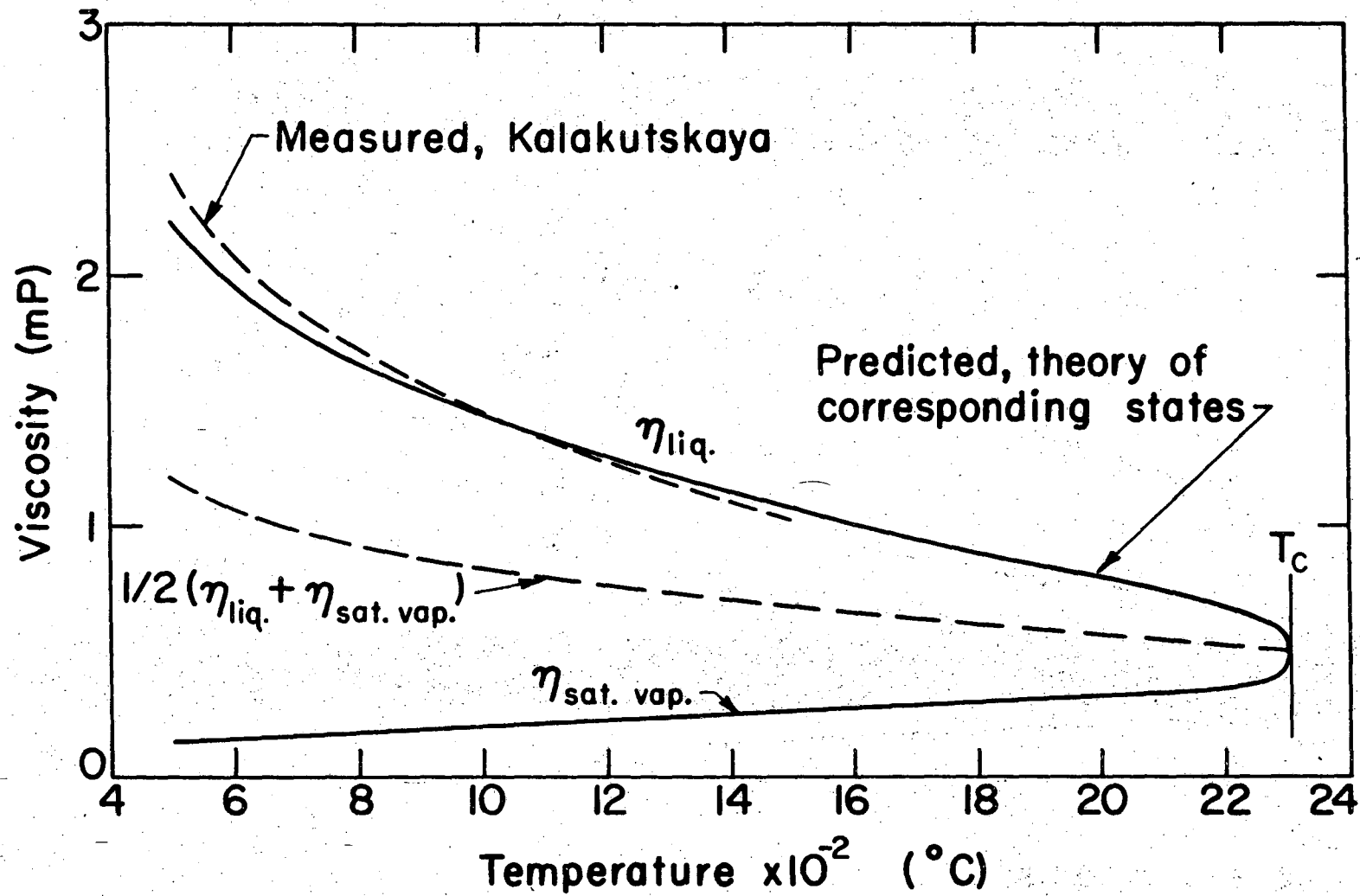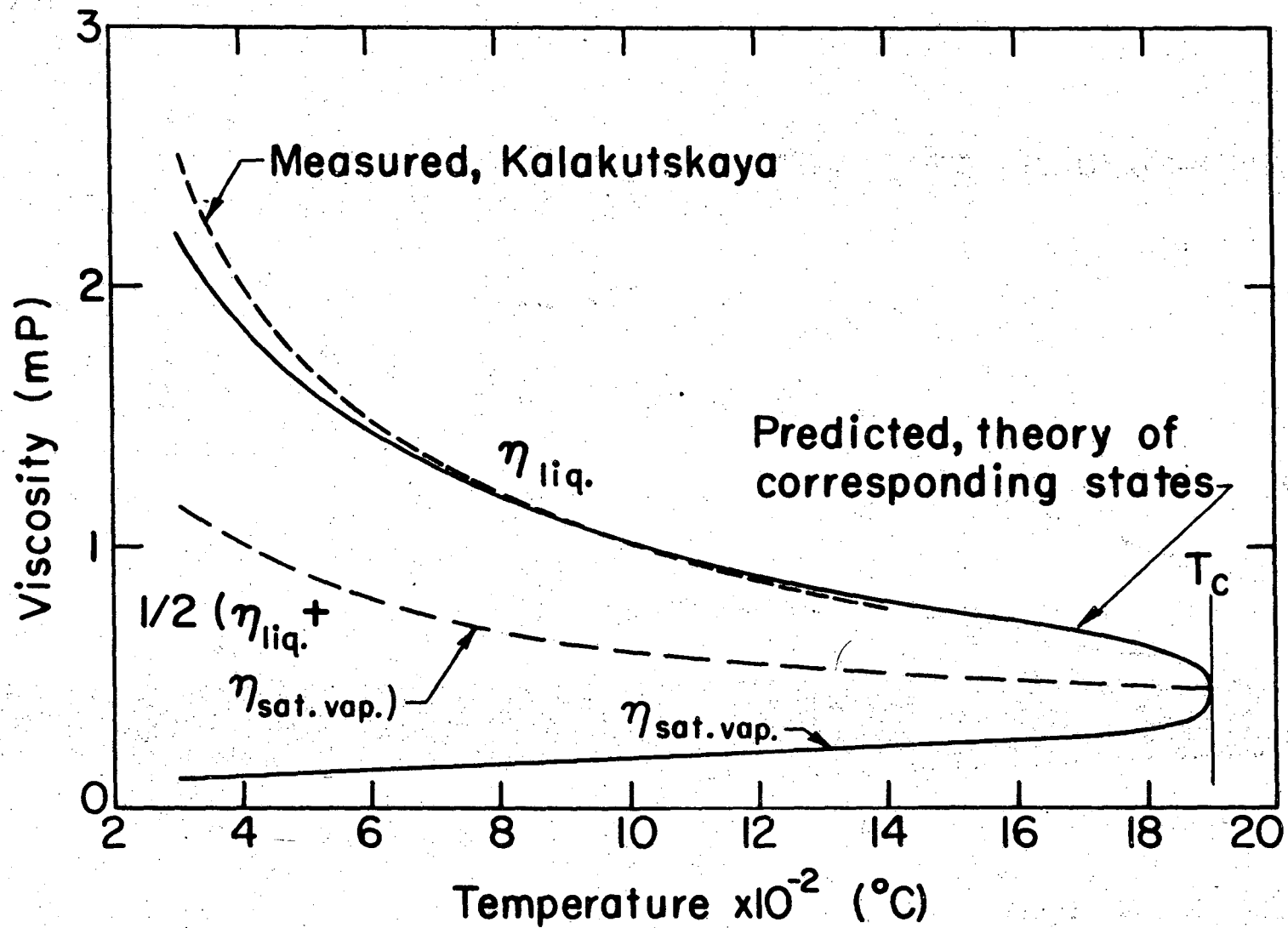
Fig. 7

Fig. 8

XBL734-2705

XBL 734-2707

Fig. 9

Fig. 10

XBL734-2700

XBL734-2699

Fig. 11